Estimation of Primary Channel Activity Statistics in Cognitive Radio Based on Imperfect Spectrum Sensing

Ogeen H. Toma, *Student Member, IEEE*, Miguel López-Benítez, *Senior Member, IEEE*, Dhaval K. Patel, *Member, IEEE*, and Kenta Umebayashi, *Member, IEEE*

***Abstract*—Primary channel statistics have recently gained increasing attention due to its remarkable role in the performance improvement of Dynamic Spectrum Access (DSA)/Cognitive Radio (CR) systems. These statistics can be calculated from the outcomes of spectrum sensing, which is the well-known method used to identify the available instantaneous opportunities in the spectrum. Computing statistical information from spectrum sensing, however, may sometimes be unreliable due to the fact that spectrum sensing is imperfect in the real world and errors are likely to occur in the sensing decisions. In this context, this work provides a detailed analysis of a broad range of primary channel statistics under Imperfect Spectrum Sensing (ISS) and finds a set of closed-form expressions for the calculated statistics under ISS as a function of the original primary channel statistics, probability of error, and the employed sensing period. In addition, the obtained mathematical expressions are employed to find and propose novel estimators for the primary channel statistics, which outperform the existing estimators in the literature and can provide accurate estimations of the original statistics even under high probability of error of spectrum sensing. The correctness of the obtained analytical expressions and the accuracy of the proposed estimators are corroborated with both simulation and experimental results.**

***Index Terms*—Cognitive radio, dynamic spectrum access, primary activity statistics, spectrum sensing.**

I. Introduction

THE spectrum scarcity problem has been exacerbated by continuing developments in the wireless communication technology while using the same limited amount of electromagnetic spectrum resource. The inefficient use and management of the radio spectrum has further increased the challenge to provide the bandwidth required by emerging technologies such as the Internet of Things (IoT), which is expected to support a myriad of wirelessly interconnected devices in the coming few years [1]. In addition, it has been reported by several international regulatory bodies, including the Federal Communications Commission (FCC) in the USA and the Office of Communications (Ofcom) in the UK, that the majority of the allocated spectrum bands are significantly underutilised due to an old-fashioned policy based on a fixed spectrum allocation [1], [2]. Dynamic Spectrum Access (DSA) [3] based on the Cognitive Radio (CR) [4] concept was introduced as a revolutionary solution to provide high spectrum utilization for wireless communications and meet the ever-increasing demand for spectrum. In DSA/CR systems, the frequency spectrum will be exploited dynamically instead of allocating different bands statically for particular wireless services, in which secondary (unlicensed) users (SUs) will be permitted to use the frequency channels of the spectrum opportunistically when the primary (licensed) users (PUs) are absent within their allocated channels, so as to ensure that no harmful interference will occur between SUs and PUs. The focus of this work is on interweave spectrum sharing where SUs are interested in the available opportunities in the time domain of the primary channels [4].

SUs in DSA/CR systems are required to have spectrum awareness about the activity and inactivity patterns of the primary channels in order to know when (i.e., the time instants) and where (i.e., the frequency channels) they can access the primary spectrum or must vacate it upon the return of PUs. Spectrum sensing is one of the methods used to provide spectrum awareness to DSA/CR systems, by which the instantaneous state of the primary channel is sensed directly by the SUs and a binary decision (either idle or busy) is made at each sensing event. Sensing decisions are made based on a predefined signal processing algorithm such as the widely used energy detection (ED) method [5]–[7], and they are directly affected by the Signal to Noise Ratio (SNR) of the sensed PUs signals. Therefore, when the detected PU signal is sufficiently strong (i.e., high SNR), Perfect Spectrum Sensing (PSS) can be achieved. However, in reality DSA/CR devices are more likely to operate under low SNR conditions and therefore errors will often occur in the sensing decisions, which leads to an Imperfect Spectrum Sensing (ISS) scenario.

This work was supported by the British Council under UKIERI DST Thematic Partnerships 2016-17 (grant ref. DST-198/2017). The work of K. Umebayashi was supported by the European Commission in the framework of the H2020-EUJ-02-2018 project 5G-Enhance (Grant agreement no. 815056) and the Ministry of Internal Affairs and Communications (MIC) of Japan.

O. H. Toma is with the Department of Electrical Engineering and Electronics, University of Liverpool, Liverpool L69 3GJ, U.K. (email: ogeen.toma@liverpool.ac.uk).

M. López-Benítez is with the Department of Electrical Engineering and Electronics, University of Liverpool, Liverpool L69 3GJ, U.K., and also with the ARIES Research Centre, Antonio de Nebrija University, 28040 Madrid, Spain (e-mail: m.lopez-benitez@liverpool.ac.uk).

D. K. Patel is with the School of Engineering and Applied Science, Ahmedabad University, Ahmedabad 380009, India (email: dhaval.patel@ahduni.edu.in).

K. Umebayashi is with the Graduate School of Engineering, Tokyo University of Agriculture and Technology, Koganei 184-8588, Japan (e-mail:ume_k@cc.tuat.ac.jp).

This work was presented in part at the 2019 IEEE Global Communications Conference (GLOBECOM).

In addition to observing the instantaneous status of the primary channel, sensing decisions can further be exploited to provide a broad range of statistical information about the primary channels. Primary channel statistics have recently gained increasing attention due to its remarkable role in the performance improvement of DSA/CR systems, and they can find a wide range of applications in wireless communication networks [8]–[10]. The utilization of these statistics include, but is not limited to:

- Spectrum prediction [11]–[14], in which the historical statistical data of the spectrum can be exploited, using various spectrum prediction algorithms (e.g., machine learning [12]), to predict or infer the future behaviour of the PUs and thus their spectrum activity.
- Spectrum sensing [15], in which an appropriate threshold for energy detection of the spectrum sensing can be selected based on the statistical information.
- Channel selection [16]–[19], in which DSA/CR systems can exploit the statistical parameters of the primary channels to select the most appropriate one that can be offered to the SUs.
- Radio resource management decisions [20]–[22], in which statistical information can also help DSA/CR systems to take decisions to mitigate the interference between PUs and SUs, optimise the system performance and enhance the utilization of the spectrum.

Since channel statistics are estimated from the outcomes of spectrum sensing, they may differ from the original statistics of the channel. Under high SNR conditions (i.e., under PSS), reasonable accuracy can be obtained, which is only affected by the time resolution imposed by the used sensing period [23]. On the other hand, under low SNR conditions (i.e., under ISS) channel statistics can significantly be inaccurately estimated due to the presence of errors in the spectrum sensing observations.

In the literature, primary channel statistics have been analysed under PSS (as in the recent work [23]) more comprehensively than under ISS. The majority of existing work where ISS has been considered has only focused on the estimation of the channel duty cycle (DC) (e.g., [24]–[26]), paying less attention to other equally important statistical properties of the primary channel. Few studies (e.g., [27]–[29]) have also considered the mean of the idle/busy periods of the primary channel, but they are constrained to a typically (exponential) distribution to model the idle/busy periods, which in practical scenarios is not a realistic assumption [30]. In this context, reconstruction techniques have been proposed to improve the estimation of the primary channel statistics under ISS [31]–[33]. These works however suffer from the following limitations: 1) no closed-form expressions are provided for these statistics, only heuristic estimation methods in the form of algorithms, and 2) the employed reconstruction algorithms assume perfect knowledge about some of the primary channel parameters (e.g., the minimum idle/busy period). The limitations of previous works and the lack of a comprehensive research work in the literature that analyses a wider range of primary channel statistics under ISS motivates this work, where a detailed analysis for various statistical parameters of the primary channel under ISS is carried out and a relation between the estimated statistics under ISS and the original statistics is provided in closed-form without introducing any constraints or requiring any prior-knowledge on the primary channel activity. The contribution of this work can therefore be highlighted as follows:

1) A set of closed-form expressions is developed for the statistics calculated under ISS as a function of the original primary statistics, probability of error, and the employed sensing period. The obtained expressions are useful in DSA/CR systems since they can provide insights on how spectrum sensing configurations can affect the estimation of statistics in the presence of sensing errors.
2) A set of novel estimators is proposed to accurately estimate the primary channel statistics even under high probability of error. The proposed estimators outperform the conventional methods proposed in the literature to estimate the statistics of the primary channel.
3) The derived analytical results for the estimated statistics and the proposed estimators are both validated by means of simulations and hardware experiments.

The remainder of this work is organised as follows. First, Section II introduces the system model considered in this work. Section III provides an explanation about the analysis procedures followed in this work to analyse primary channel statistics. Afterwards, a broad range of statistical parameters are analysed including the minimum period (Section IV), the mean period (Section V), the channel duty cycle (Section VI) and the distribution of the periods (Section VII), where novel analytical results and estimators are obtained. The correctness of the conducted analysis for the statistical parameters, including the closed-form expressions and the novel estimators, is validated by means of simulations and hardware experiments in Section VIII. Finally, conclusions are drawn in Section IX.

II. System Model

We consider a single primary channel which is occupied by a PU and this occupation is represented by a sequence of idle/busy periods in the time-domain. The idle and busy times can be modelled to follow a particular distribution that according to the experimental measurements in [30] can be accurately described by a Generalised Pareto (GP) distribution. In our analysis, however, this information will be considered to be unknown to the DSA/CR system. By performing spectrum sensing, DSA/CR systems will try to estimate the duration of the idle/busy periods of a primary channel. This is achieved by observing the state of the channel periodically at a constant time interval referred to as the sensing period T_s. At every sensing event a binary decision is made, either $\mathcal{H}_0$ to represent the idle state or $\mathcal{H}_1$ to represent the busy state of the PU channel. As a result, the output of spectrum sensing will be a set of binary decisions. Based on these decisions the idle/busy periods of a primary channel can be estimated. When the channel state toggles from idle to busy or reversely, the time interval elapsed since the last toggle will be calculated as $\widehat{T}_i$ to represent the PSS estimation of the real periods T_i

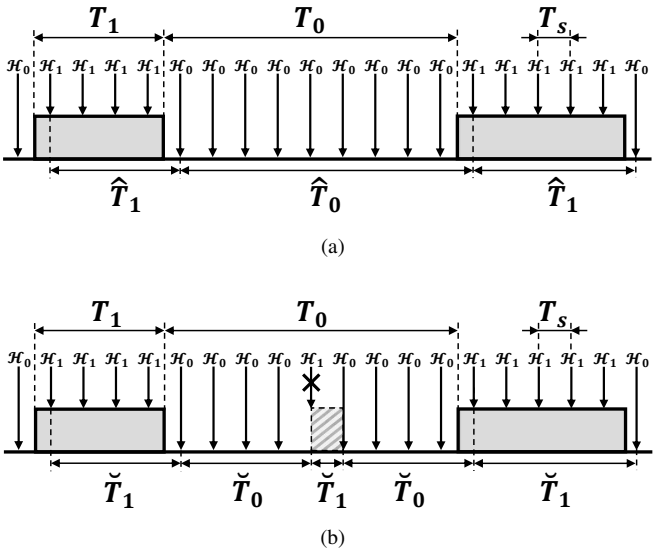

Fig. 1: Estimation of idle/busy periods based on spectrum sensing: (a) under perfect spectrum sensing (PSS), (b) under imperfect spectrum sensing (ISS) [31].

(where i refers to the type of the period, $i = 0$ for idle and $i = 1$ for busy), as shown in Fig. 1(a). This estimation provides a reasonable level of accuracy for the individual periods of T_i when no errors are assumed to occur in the sensing events $\mathcal{H}_i$ (i.e., the accuracy is only affected by the time resolution T_s of the periodic sensing events). However, occasional errors in the sensing events $\mathcal{H}_i$ are likely to occur in practice, especially under low SNR conditions. These errors can be categorised into two types: false alarms (which occur when an idle state of the channel is reported as a busy state) and missed detections (which occur when a busy state of the channel is reported as an idle state). The estimated periods in the presence of the sensing errors are denoted as $\check{T}_i$ to represent the ISS estimation of the real periods T_i as shown in Fig. 1(b), where the impact of a false alarm is illustrated. Sensing errors can be modelled as i.i.d. random variables for each sensing event with a fixed probability of false alarm P_{fa} and a fixed probability of missed detection P_{md}, which is a common modelling approach in the DSA/CR literature. The value of these probabilities in a practical scenario will depend on the system's operating conditions as well as the configuration of the employed spectrum sensing algorithm, which is an algorithm-specific problem and therefore is out of the scope of this work. However, the system designer can always know how a particular sensing algorithm will behave in terms of these error probabilities (e.g., in an energy detector these probabilities can be easily related to the selected energy decision threshold). Therefore, these probabilities can be assumed to be known in practice. The characterisation of the spectrum sensing algorithm performance in terms of its false alarm and missed detection probabilities makes the analysis presented in this work valid irrespective of the specific spectrum sensing algorithm implemented in the DSA/CR system.

III. Estimation of the Primary Channel Activity Statistics Under ISS

DSA/CR systems can estimate the idle/busy periods of the primary channel by using spectrum sensing decisions. Based on a sufficiently large set of such periods [34], DSA/CR systems can also obtain the statistical information of the primary channel activity. Since this work is concerned with the estimation of the primary activity statistics in the presence of sensing errors (i.e., considering a realistic spectrum sensing scenario), the set of idle/busy periods observed under ISS, as shown in Fig. 1(b), is the one considered in this work for statistics calculations. Therefore, a set $\{\check{T}_{i,n}\}_{n=1}^{N_{iss}}$ of N_{iss} periods observed under ISS is used to estimate the statistical parameters of the primary channel.

The idle/busy period durations $\check{T}_i$ observed under ISS are affected by several configuration parameters of the spectrum sensing algorithm. These parameters include the employed sensing period T_s and the selected value of probability of error (i.e., P_{fa} and P_{md}), which in the case of ED depend on the selected energy decision threshold [5]–[7]. The estimation of the primary activity statistics under ISS, therefore, can be analysed based on these parameters and a relationship between the statistics estimated under ISS and the original statistics can be found as a function of T_s, P_{fa} and P_{md}. Note that the analysis of the sample size parameter N_{iss}, which represents the number of idle/busy periods used to calculate the statistics, is out of the scope of this work and therefore it will be assumed to be sufficiently large to provide accurate results.

In order to find a mathematical relationship between the statistics estimated under ISS and the original statistics of the primary channel, three stages of analysis are required:

1) Finding a relationship between the statistics estimated under ISS and the statistics estimated under PSS.
2) Finding a relationship between the statistics estimated under PSS and the original statistics.
3) Combining the second relationship with the first one results in the desired relationship (i.e., the relationship between the statistics estimated under ISS and the original statistics).

The relationship obtained in the first stage of this analysis should be as a function of the sensing period T_s, P_{fa}, and P_{md} as mentioned above, while the relationship in the second stage should only be as a function of the sensing period T_s as PSS is assumed with no sensing errors (i.e., $P_{fa} = P_{md} = 0$). Since the second relationship (i.e., between the statistics estimated under PSS and the original statistics) has already been analysed in [23], this work focuses on the analysis of the first relationship (i.e., between the statistics estimated under ISS and the statistics estimated under PSS), which has not been covered yet in the literature. Furthermore, the final relationship between the statistics estimated under ISS and the original statistics will then be achieved by combining the analysis presented in [23] with the analysis carried out in this work, which considers the same set of statistical metrics as in [23], namely the minimum period, mean of periods, duty cycle, and distribution of the estimated periods.

IV. Estimation of the Minimum Period

The minimum period μ_i of a primary channel is the shortest time that a primary channel can be active or inactive. This parameter can help determine the minimum opportunistic time that can be exploited by the SUs, or the minimum time that the SUs need to wait until a new opportunity becomes available in the primary channel. DSA/CR systems can estimate the minimum period μ_i of the channel from spectrum sensing observations. Although this parameter has already been studied in [23] under PSS and in [31] under ISS, we summarise the analysis here in order to make this work self-contained.

Based on a given set $\{\widehat{T}_{i,n}\}_{n=1}^{N_{pss}}$ of N_{pss} periods observed under PSS, [23] found that the estimated minimum period $\widehat{\mu}_i$ under PSS can be expressed as a function of the original minimum period μ_i and sensing period $T_s \leq \mu_i$ as [23, eq. (7)]:

$$\widehat{\mu}_i = \min\left(\{\widehat{T}_{i,n}\}_{n=1}^{N_{pss}}\right) = \left\lfloor \frac{\mu_i}{T_s} \right\rfloor T_s, \qquad T_s \leq \mu_i, \tag{1}$$

where $\lfloor\cdot\rfloor$ denotes the floor operator. As it can be appreciated from (1), the minimum period can be correctly estimated under PSS (i.e., $\widehat{\mu}_i = \mu_i$) when T_s is an integer submultiple of the true minimum (i.e., when $T_s = \mu_i/k$, $k \in \mathbb{N}^+$), otherwise $\widehat{\mu}_i < \mu_i$ [23]. On the other hand, the minimum period cannot be estimated correctly under ISS because the minimum observed period would be equal to the duration of a single sensing error, which in turn is equal to the sensing period T_s [31], no matter how low the probability of error is. Therefore, from a given set $\{\breve{T}_{i,n}\}_{n=1}^{N_{iss}}$ of N_{iss} periods observed under ISS, the minimum estimated period would be [31]:

$$\breve{\mu}_i = \min\left(\{\breve{T}_{i,n}\}_{n=1}^{N_{iss}}\right) = T_s. \tag{2}$$

As it can be noticed from the observed periods under ISS in Fig. 1(b), the minimum busy (idle) period would be the duration of the single false alarm (missed detection), which is equal to T_s (the same applies to missed detections during busy periods). Since (2) shows that the estimated minimum period under ISS is solely dependent on the sensing period T_s (regardless of the original value of the minimum), it is impossible to find, from this expression, an exact relationship between the estimated minimum period $\breve{\mu}_i$ under ISS and the original minimum μ_i.

V. Estimation of the Mean Period

A. Relationship Between the Mean Estimated Under ISS and the Original Mean

One of the main statistical moments of the primary channel activity is the mean of the idle/busy periods. For a given set $\{\widehat{T}_{i,n}\}_{n=1}^{N_{pss}}$ of N_{pss} periods estimated under PSS, the mean $\mathbb{E}(\widehat{T}_i)$ of the observed periods can be found by using the conventional (unbiased) sample mean estimator $\widehat{m}_i$:

$$\mathbb{E}(\widehat{T}_i) \approx \widehat{m}_i = \frac{1}{N_{pss}} \sum_{n=1}^{N_{pss}} \widehat{T}_{i,n}. \tag{3}$$

The analysis in [23] has shown that the estimated mean under PSS is approximately equal to the true mean of the channel periods (i.e., $\widehat{m}_i \approx \mathbb{E}(T_i)$). However, this does not apply to the estimated mean under ISS because when an error occurs in the sensing decisions (either false alarm or missed detection), it will divide the original period duration T_i into shorter fragments. As it can be noticed in Fig. 1(b), a single false alarm error could corrupt the estimation of an idle period T_0 period by dividing it into three new shorter periods, which are $\breve{T}_0, \breve{T}_1$, and $\breve{T}_0$. The duration of the $\breve{T}_1$ fragment is equal to the sensing period T_s, while the durations of the two $\breve{T}_0$ fragments are random, depending on the position of the error itself within T_0.

Due to this phenomenon, the number of the observed periods under ISS (N_{iss}) would not be the same as the number of the periods observed under PSS (N_{pss}). As shown in Fig. 1(b), with a single false alarm, the original T_0 period is estimated as two $\breve{T}_0$ periods and one $\breve{T}_1$ period. If there were two false alarms within T_0, then they would result in three $\breve{T}_0$ and two $\breve{T}_1$ periods, and so on. Therefore, each false alarm would produce an additional estimated idle period $\breve{T}_0$ and an additional estimated busy period $\breve{T}_1$ (a similar effect would be observed with missed detections). As a result, the number N_{iss} of periods observed under ISS will be greater than the actual number of the periods N (unlike under PSS where no additional periods are produced during the spectrum sensing process and thus $N_{pss} = N$). Therefore, from a given set $\{\breve{T}_{i,n}\}_{n=1}^{N_{iss}}$ of N_{iss} periods estimated under ISS, the mean calculated using the following conventional mean estimator:

$$\mathbb{E}(\breve{T}_i) \approx \breve{m}_i = \frac{1}{N_{iss}} \sum_{n=1}^{N_{iss}} \breve{T}_{i,n} \tag{4}$$

would be highly inaccurate (indeed, much lower than the original value of the mean). In order to find the relationship between the mean calculated under ISS $\mathbb{E}(\breve{T}_i)$ and the original value of the mean $\mathbb{E}(T_i)$ of the channel periods, we first find its relationship with the mean calculated under PSS $\mathbb{E}(\widehat{T}_i)$ as discussed in Section III. The analysis will consider first, without loss of generality, the sample mean for idle periods (i.e., $\breve{m}_0$, $\breve{m}_i$ with $i = 0$), and will be later on generalised to both idle and busy periods. We start by taking the primary channel periods illustrated in Fig. 1(b) as an example, which leads to the following estimated mean idle period:

$$\breve{m}_0 = \frac{1}{2}\sum_{n=1}^{2} \breve{T}_{0,n} = \frac{\breve{T}_{0,1} + \breve{T}_{0,2}}{2} = \frac{\widehat{T}_0 - \breve{T}_1}{2} = \frac{\widehat{T}_0 - T_s}{2}.$$

The mean of the idle periods in Fig. 1(b) is the summation of the two idle periods ($\breve{T}_{0,1}$ and $\breve{T}_{0,2}$) divided by 2. This summation is equivalent to subtracting $\breve{T}_1$ from the estimated period $\widehat{T}_0$ under PSS, knowing that the produced $\breve{T}_1$ period from the false alarm error is equal to the sensing period T_s. In addition, the denominator 2, which represents the number of the estimated idle periods under ISS (i.e., N_{iss}), can be substituted with the number of estimated idle periods under PSS plus one for the single false alarm (i.e., $N_{iss} = N_{pss} + 1$). This analysis of a single false alarm error within a single idle period can be extended to a general form for any arbitrary

number of false alarm errors within the whole set of idle periods as:

$$\breve{m}_0 = \frac{\sum_{n=1}^{N_{pss}} \widehat{T}_{0,n} - N_{fa}T_s}{N_{pss} + N_{fa}}, \tag{5}$$

where N_{fa} represents the total number of false alarm errors in the entire set of observed periods, which can be found by multiplying the entire number of $\mathcal{H}_0$ events (i.e., idle sensing decisions) by the probability of false alarm P_{fa} as:

$$N_{fa} = \frac{\sum_{n=1}^{N_{pss}} \widehat{T}_{0,n}}{T_s} \cdot P_{fa}. \tag{6}$$

The above analysis has assumed no missed detection errors in the sensing decisions of the channel periods (i.e., $P_{md} = 0$). However, missed detections will also lead to the presence of some idle periods in the observed set. In order to find $\breve{m}_0$ by taking into consideration the missed detections as well, a similar logic can be followed so that (5) can be rewritten to include both sensing error types:

$$\breve{m}_0 = \frac{\sum_{n=1}^{N_{pss}} \widehat{T}_{0,n} - N_{fa}T_s + N_{md}T_s}{N_{pss} + N_{fa} + N_{md}}, \tag{7}$$

where N_{md} represents the total number of missed detection errors in the entire set of observed periods, which can be found by multiplying the entire number of $\mathcal{H}_1$ events (i.e., busy sensing decisions) by the probability of missed detection P_{md} as:

$$N_{md} = \frac{\sum_{n=1}^{N_{pss}} \widehat{T}_{1,n}}{T_s} \cdot P_{md}. \tag{8}$$

By substituting (6) and (8) in (7):

$$\breve{m}_0 = \frac{\sum_{n=1}^{N_{pss}} \widehat{T}_{0,n} - \frac{\sum_{n=1}^{N_{pss}} \widehat{T}_{0,n}}{T_s} \cdot P_{fa}T_s + \frac{\sum_{n=1}^{N_{pss}} \widehat{T}_{1,n}}{T_s} \cdot P_{md}T_s}{N_{pss} + \frac{\sum_{n=1}^{N_{pss}} \widehat{T}_{0,n}}{T_s} \cdot P_{fa} + \frac{\sum_{n=1}^{N_{pss}} \widehat{T}_{1,n}}{T_s} \cdot P_{md}}. \tag{9}$$

Note that from (3), the term $\sum_{n=1}^{N_{pss}} \widehat{T}_{i,n}$ can be written as:

$$\sum_{n=1}^{N_{pss}} \widehat{T}_{i,n} = N_{pss}\widehat{m}_i. \tag{10}$$

Therefore, using (10), expression (9) can be further simplified to:

$$\breve{m}_0 = \frac{\widehat{m}_0(1 - P_{fa}) + \widehat{m}_1 P_{md}}{1 + \frac{\widehat{m}_0}{T_s}P_{fa} + \frac{\widehat{m}_1}{T_s}P_{md}}. \tag{11}$$

Although this equation can provide a mathematical relationship between the calculated mean under ISS, $\breve{m}_0$, and the calculated mean under PSS, $\widehat{m}_0$, it lacks some accuracy. The reason is that there are some particular cases where sensing errors (either false alarms or missed detections) will not produce additional estimated idle periods ($\breve{T}_0$) and additional estimated busy periods ($\breve{T}_1$). This will be analysed in the following two particular cases.

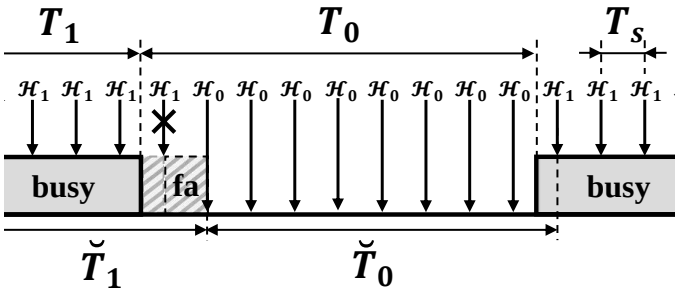

Fig. 2: Case I: A single sensing error at the edge of a period.

*1) **Case I**:* When a sensing error occurs at the edge of the idle/busy period being estimated, the error period itself will be adjacent to an actual idle/busy period. As a result, there will be no additional fragments produced from such sensing error (i.e., such error will only affect the duration of the estimated periods). As shown in Fig. 2, the false alarm at the left edge of the idle period is combined with the adjacent busy period and both together are estimated as a single $\breve{T}_1$ period. Therefore, there will be no additional $\breve{T}_0$ or $\breve{T}_1$ fragments produced from such false alarm. The previous analysis has assumed that all the sensing errors will produce an additional idle period and an additional busy period without considering the case explained here. To include this effect, the denominator in (7), which represents the number of the estimated periods under ISS ($N_{iss} = N_{pss} + N_{fa} + N_{md}$), should not count the cases when the sensing errors occur at the edges of the periods since there will be no additional periods produced by them. This can be attained by knowing that each estimated idle/busy period will have two edges and these edges are actually represented by sensing events $\mathcal{H}_0$/$\mathcal{H}_1$. Therefore, the problem in the denominator of (7) and the resulting (11) can be solved by subtracting the two sensing events for both edges from the total number of sensing events within a single period (or $2N_{pss}$ from the entire number of the events within N_{pss} periods), and thus (11) can be corrected to yield:

$$\breve{m}_0 = \frac{\widehat{m}_0(1 - P_{fa}) + \widehat{m}_1 P_{md}}{1 + \left(\frac{\widehat{m}_0}{T_s} - 2\right) P_{fa} + \left(\frac{\widehat{m}_1}{T_s} - 2\right) P_{md}}. \tag{12}$$

*2) **Case II**:* It is also possible that some sensing errors will not produce additional periods when they occur in bursts (i.e., they are consecutive to other errors). Fig. 3 shows how two false alarms could occur consecutively in the sensing decisions of an idle period. Although most of the sensing errors could occur as individual periods (with a duration equal to T_s), it is still possible, depending on the probability of errors, to observe some occasional consecutive errors in the sensing decisions. However, the probability of having two consecutive errors is higher than that of having three or more consecutive errors as also illustrated in [33, Fig. 3]. Consecutive errors will have the same effect of a single error in terms of the number of produced fragments. For example, the resulting fragments of the two consecutive false alarms in Fig. 3 are $\breve{T}_0$, $\breve{T}_1$, and $\breve{T}_0$, which is the same number of the resulting fragments from a single false alarm observed in the example of Fig. 1(b). Since

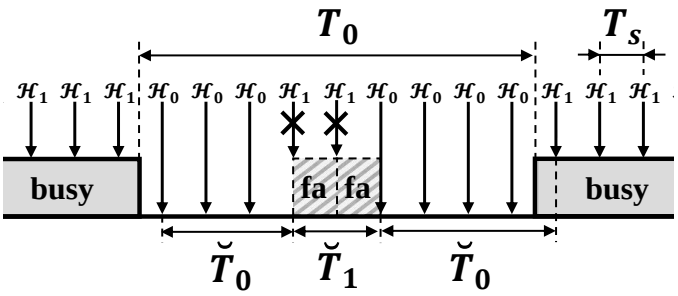

Fig. 3: Case II: Two consecutive sensing errors in the middle of a period.

there are no additional fragments resulting from consecutive errors, the denominator of (7) should therefore not count these errors. This can be attained by subtracting the probability of having consecutive errors from the probability of error itself. As a result, P_{fa} and P_{md} used in (6) and (8) to find N_{fa} and N_{md} should be modified as follows:

$$\grave{P}_{fa} = P_{fa} - \sum_{j=2}^{\infty} P_{fa}^{j} = P_{fa}\left(\frac{1-2P_{fa}}{1-P_{fa}}\right), \tag{13}$$

where $\grave{P}_{fa}$ represents the probability of having false alarms as separate periods, irrespective of being consecutive or isolated errors, and the relation $\sum_{j=2}^{\infty} a^j = \frac{a^2}{1-a}$, when $|a| < 1$ has been used to obtain the final expression in (13). This also applies to the consecutive missed detection errors, hence:

$$\grave{P}_{md} = P_{md} - \sum_{j=2}^{\infty} P_{md}^{j} = P_{md}\left(\frac{1-2P_{md}}{1-P_{md}}\right). \tag{14}$$

- ***Final closed-form expression of the mean:***

Taking into account these two special cases, the final expression for the estimated mean idle period under ISS, $\breve{m}_0$, is obtained by introducing (13) and (14) into the denominator of (12), which yields the final analytical result:

$$\breve{m}_0 = \frac{\widehat{m}_0(1-P_{fa}) + \widehat{m}_1 P_{md}}{1 + \left(\frac{\widehat{m}_0}{T_s} - 2\right)\grave{P}_{fa} + \left(\frac{\widehat{m}_1}{T_s} - 2\right)\grave{P}_{md}}. \tag{15}$$

The achieved expression in (15) provides the relationship between the mean $\breve{m}_0$ estimated under ISS (for idle periods) and the means $\widehat{m}_i$ estimated under PSS (for both idle and busy periods), which satisfies the first stage of the analysis as mentioned in Section III. On the other hand, the relationship between the mean $\widehat{m}_i$ estimated under PSS and the original mean m_i was already analysed in [23], which shows that the population mean of the periods observed under PSS is exactly equal to the population mean of the original periods (i.e., $\mathbb{E}(\widetilde{T}_i) = \mathbb{E}(T_i)$), thus providing the second stage of the analysis as mentioned in Section III. Therefore, by assuming a sufficiently large sample size (i.e., number of periods), the sample means in (15) can be substituted by population means so that the second relationship can be combined with the first one to obtain the desired relationship between the estimated mean under ISS and the original mean, which completes the third stage of the analysis mentioned in Section III as:

$$\mathbb{E}(\breve{T}_0) = \frac{\mathbb{E}(T_0)(1-P_{fa}) + \mathbb{E}(T_1)P_{md}}{1 + \left(\frac{\mathbb{E}(T_0)}{T_s} - 2\right)\grave{P}_{fa} + \left(\frac{\mathbb{E}(T_1)}{T_s} - 2\right)\grave{P}_{md}}. \tag{16}$$

A similar analysis can also be followed to find the estimated mean of the busy periods $\mathbb{E}(\breve{T}_1)$. Therefore, the final closed-form expression for the estimated mean of the idle/busy periods $\mathbb{E}(\breve{T}_i)$ under ISS can be expressed in a compact form as:

$$\mathbb{E}(\breve{T}_i) = \frac{\mathbb{E}(T_i) - (-1)^i\,\mathbb{E}(T_0)P_{fa} + (-1)^i\,\mathbb{E}(T_1)P_{md}}{1 + \left(\frac{\mathbb{E}(T_0)}{T_s} - 2\right)\grave{P}_{fa} + \left(\frac{\mathbb{E}(T_1)}{T_s} - 2\right)\grave{P}_{md}}, \tag{17}$$

which provides the final expression for the estimated mean $\mathbb{E}(\breve{T}_i)$ under ISS as a function of the original mean $\mathbb{E}(T_i)$, probabilities of error P_{fa} and P_{md}, and sensing period T_s.

B. Mean Estimation Method

The closed-form expression obtained in (17), which provides a mathematical relationship between the estimated mean under ISS and the original mean, suggests a novel method to accurately estimate the original mean of the channel periods from the outcomes of the ISS estimates. In this section we propose a novel method to accurately estimate the original value of the mean of the idle/busy periods from the ISS observations. The analytical result in (17) summarises two expressions, namely the estimated mean of idle periods under ISS (when $i = 0$) and the estimated mean of busy periods under ISS (when $i = 1$), which can be rewritten in explicit form as:

$$\mathbb{E}(\breve{T}_0) = \frac{\mathbb{E}(T_0) - \mathbb{E}(T_0)P_{fa} + \mathbb{E}(T_1)P_{md}}{1 + \left(\frac{\mathbb{E}(T_0)}{T_s} - 2\right)\grave{P}_{fa} + \left(\frac{\mathbb{E}(T_1)}{T_s} - 2\right)\grave{P}_{md}}, \tag{18}$$

$$\mathbb{E}(\breve{T}_1) = \frac{\mathbb{E}(T_1) + \mathbb{E}(T_0)P_{fa} - \mathbb{E}(T_1)P_{md}}{1 + \left(\frac{\mathbb{E}(T_0)}{T_s} - 2\right)\grave{P}_{fa} + \left(\frac{\mathbb{E}(T_1)}{T_s} - 2\right)\grave{P}_{md}}. \tag{19}$$

The above two expressions can be solved for the original mean periods (i.e., $\mathbb{E}(T_0)$ and $\mathbb{E}(T_1)$) as shown in (20) and (21), respectively. By substituting (21) in (20), a new expression can be derived in (22), denoted as $\mathbb{E}(\widetilde{T}_0)$, to represent the accurate estimation of the original mean $\mathbb{E}(T_0)$ as a function of the estimated mean under ISS (i.e., $\mathbb{E}(\breve{T}_0)$ and $\mathbb{E}(\breve{T}_1)$), probability of errors (i.e., P_{fa} and P_{md}), and sensing period (i.e., T_s). Similarly, the estimator for the mean of the busy periods $\mathbb{E}(\widetilde{T}_1)$ can be derived by substituting (20) in (21). The final expression for the mean estimator of the idle/busy periods $\mathbb{E}(\widetilde{T}_i)$ can be written in compact form as shown in (24).

The result in (24) represents a novel method to accurately estimate the original value of the mean of the channel periods based on the estimated mean under ISS, probabilities of error, and sensing period. It is worth mentioning that the probabilities of error P_{fa} and P_{md}, and sensing period T_s are all configured based on the spectrum sensing algorithm used by the CR system and are known. Therefore, this method is applicable in real hardware implementations, as opposed to most previous estimation methods proposed in the existing literature.

$$\mathbb{E}(T_0) = \mathbb{E}(\check{T}_0)\frac{1-2\grave{P}_{fa}-2\grave{P}_{md}}{1-P_{fa}-\frac{\grave{P}_{fa}}{T_s}\mathbb{E}(\check{T}_0)} + \mathbb{E}(T_1)\frac{\frac{\grave{P}_{md}}{T_s}\mathbb{E}(\check{T}_0)-P_{md}}{1-P_{fa}-\frac{\grave{P}_{fa}}{T_s}\mathbb{E}(\check{T}_0)} \tag{20}$$

$$\mathbb{E}(T_1) = \mathbb{E}(\check{T}_1)\frac{1-2\grave{P}_{fa}-2\grave{P}_{md}}{1-P_{md}-\frac{\grave{P}_{md}}{T_s}\mathbb{E}(\check{T}_1)} + \mathbb{E}(T_0)\frac{\frac{\grave{P}_{fa}}{T_s}\mathbb{E}(\check{T}_1)-P_{fa}}{1-P_{md}-\frac{\grave{P}_{md}}{T_s}\mathbb{E}(\check{T}_1)} \tag{21}$$

$$\mathbb{E}(T_0) \approx \mathbb{E}(\widetilde{T}_0) = \frac{\left(\mathbb{E}(\check{T}_0)(1-P_{md}) - \mathbb{E}(\check{T}_1)P_{md}\right)\left(1-2\grave{P}_{fa}-2\grave{P}_{md}\right)}{\left(1-P_{fa}-\frac{\grave{P}_{fa}}{T_s}\mathbb{E}(\check{T}_0)\right)\left(1-P_{md}-\frac{\grave{P}_{md}}{T_s}\mathbb{E}(\check{T}_1)\right) - \left(\frac{\grave{P}_{fa}}{T_s}\mathbb{E}(\check{T}_1)-P_{fa}\right)\left(\frac{\grave{P}_{md}}{T_s}\mathbb{E}(\check{T}_0)-P_{md}\right)} \tag{22}$$

$$\mathbb{E}(T_1) \approx \mathbb{E}(\widetilde{T}_1) = \frac{\left(\mathbb{E}(\check{T}_1)(1-P_{fa}) - \mathbb{E}(\check{T}_0)P_{fa}\right)\left(1-2\grave{P}_{fa}-2\grave{P}_{md}\right)}{\left(1-P_{fa}-\frac{\grave{P}_{fa}}{T_s}\mathbb{E}(\check{T}_0)\right)\left(1-P_{md}-\frac{\grave{P}_{md}}{T_s}\mathbb{E}(\check{T}_1)\right) - \left(\frac{\grave{P}_{fa}}{T_s}\mathbb{E}(\check{T}_1)-P_{fa}\right)\left(\frac{\grave{P}_{md}}{T_s}\mathbb{E}(\check{T}_0)-P_{md}\right)} \tag{23}$$

$$\mathbb{E}(T_i) \approx \mathbb{E}(\widetilde{T}_i) = \frac{\left(\mathbb{E}(\check{T}_i)(1-P_{md}^{1-i}P_{fa}^{i}) - \mathbb{E}(\check{T}_{1-i})P_{md}^{1-i}P_{fa}^{i}\right)\left(1-2\grave{P}_{fa}-2\grave{P}_{md}\right)}{\left(1-P_{fa}-\frac{\grave{P}_{fa}}{T_s}\mathbb{E}(\check{T}_0)\right)\left(1-P_{md}-\frac{\grave{P}_{md}}{T_s}\mathbb{E}(\check{T}_1)\right) - \left(\frac{\grave{P}_{fa}}{T_s}\mathbb{E}(\check{T}_1)-P_{fa}\right)\left(\frac{\grave{P}_{md}}{T_s}\mathbb{E}(\check{T}_0)-P_{md}\right)} \tag{24}$$

VI. Estimation of the Duty Cycle

The Duty Cycle (DC), also referred to as the channel occupancy rate or the channel load, is one of the most widely used statistical metrics in DSA/CR systems due to its simplicity and applicability in enhancing the efficiency of spectrum utilization. The DC of the primary channel is traditionally estimated from the spectrum sensing observations by dividing the number of busy sensing events over the entire number of the sensing events [35]–[37]. Although this is the most widely used approach in the literature, it is highly sensitive to the presence of the sensing errors. On the other hand, and in the context of PSS, another method was proposed in [38] to estimate the DC of the primary channel denoted as Ψ, based on the mean of the idle/busy periods as:

$$\Psi = \frac{\mathbb{E}(T_1)}{\mathbb{E}(T_1)+\mathbb{E}(T_0)}. \tag{25}$$

The observed idle/busy periods $\widehat{T}_i$ under PSS can serve to obtain an accurate estimation for the mean $\mathbb{E}(\widehat{T}_i)$ and thus an accurate estimation of the DC of the primary channel as well. However, in the ISS scenario, the observed idle/busy periods $\check{T}_i$ could be significantly corrupted because of the sensing errors, as explained in Section V, and the estimated mean of these periods could be highly inaccurate. Therefore, estimating the DC of the channel under ISS as given in (26), which depends solely on the mean of the observed periods, would be highly inaccurate (i.e., $\check{\Psi} \neq \Psi$).

$$\check{\Psi} = \frac{\mathbb{E}(\check{T}_1)}{\mathbb{E}(\check{T}_1)+\mathbb{E}(\check{T}_0)} \neq \Psi. \tag{26}$$

An alternative approach is here proposed based on the analysis presented in Section V and the new mean estimator $\mathbb{E}(\widetilde{T}_i)$ in (24), which can be used to estimate the mean of the idle/busy periods accurately under ISS even when the probability of sensing error is high. This estimator can also be exploited to find the DC of the channel under ISS. Therefore, by substituting the mean estimator of (24) in (25), a new DC estimator $\widetilde{\Psi}$ is obtained as:

$$\widetilde{\Psi} = \frac{\mathbb{E}(\widetilde{T}_1)}{\mathbb{E}(\widetilde{T}_1)+\mathbb{E}(\widetilde{T}_0)} \approx \Psi, \tag{27}$$

where $\mathbb{E}(\widetilde{T}_0)$ and $\mathbb{E}(\widetilde{T}_1)$ are the accurate estimations of $\mathbb{E}(T_0)$ and $\mathbb{E}(T_1)$ provided by (22) and (23), respectively, and thus the obtained $\widetilde{\Psi}$ provides an accurate estimation of the true DC Ψ.

VII. Estimation of the Distribution

A. Relationship Between the Distribution Estimated Under ISS and the Original Distribution

The idle/busy periods observed from sensing decisions are integer multiples of the sensing period (i.e., $\check{T}_i = kT_s$, $k \in \mathbb{N}^+$) and, as discussed in Section IV, the minimum estimated period under ISS is T_s, which is due to the occurrence of isolated sensing errors. As a result, the distribution of the idle/busy periods estimated under ISS is discretely shaped with a discrete step of T_s, starting from the minimum period T_s up to the maximum multiple integer of T_s observed in the channel. In order to find a closed-form expression for the Probability Mass Function (PMF) of the idle/busy periods under ISS as a function of the original PDF, probabilities of error, and sensing period, this analysis considers, without loss of generality, the case of idle periods, introducing the false alarms first and missed detections later on, similar to the procedure followed in Section V for the estimation of the mean idle period.

- ***Impact of false alarms:***

False alarms occur in the sensing decisions of the idle periods with a probability $P_{fa} > 0$. This means that any sensing decision $\mathcal{H}_0$ within a T_0 idle period as shown in Fig. 1(b) will have a probability of P_{fa} to be a false alarm, and a probability of $1 - P_{fa}$ not to be a false alarm (i.e., to be a correct decision). Consequently, to find the PMF of idle periods under ISS, denoted as $f_{\check{T}_0}(\check{T}_0 = kT_s)$, we need to consider all the possible cases in which the observed idle

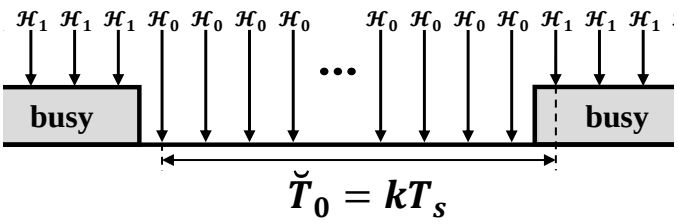

Fig. 4: Case I: An idle period $\breve{T}_0 = kT_s$ observed between two busy periods without sensing errors.

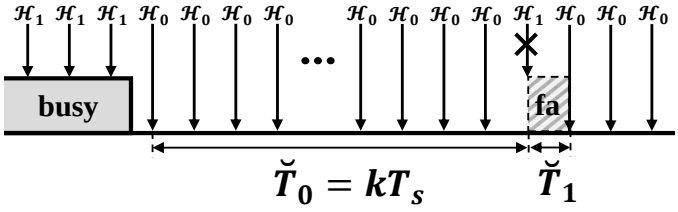

Fig. 5: Case II: An idle period $\breve{T}_0 = kT_s$ observed between a busy period and a false alarm.

periods under ISS, $\breve{T}_0 = kT_s$, could be affected by the presence of sensing errors. This can be summarised into three possible cases, which are analysed in detail below.

*1) **Case I**:* In this case, an idle period is observed between two busy periods without having any false alarms as shown in Fig. 4. The probability of having such case can be calculated as:

$$P(\breve{T}_0 = kT_s \mid \widehat{T}_0 = kT_s) = (1 - P_{fa})^k, \tag{28}$$

which is the probability of having k correct decisions in k sensing events within an idle period (i.e., k non-false alarms). To find the unconditional PMF of such periods from a set $\{\widehat{T}_{0,n}\}_{n=1}^{N_{pss}}$ of N_{pss} idle periods observed under PSS, such probability should be multiplied by the ratio N^I_{pss}/N_{iss} as follows:

$$f^I_{\breve{T}_0}(\breve{T}_0 = kT_s) = \frac{(1 - P_{fa})^k N^I_{pss}}{N_{iss}}, \tag{29}$$

where N^I_{pss} represents the number of periods observed under PSS with a duration equal to kT_s (i.e., $\widehat{T}_0 = kT_s$), which is given by $f_{\widehat{T}_0}(\widehat{T}_0 = kT_s)N_{pss}$. Thus, (29) can be written as:

$$\begin{aligned} f^I_{\breve{T}_0}(\breve{T}_0 = kT_s) &= \frac{(1 - P_{fa})^k f_{\widehat{T}_0}(\widehat{T}_0 = kT_s)N_{pss}}{N_{iss}} \\ &= \beta(1 - P_{fa})^k f_{\widehat{T}_0}(\widehat{T}_0 = kT_s), \end{aligned} \tag{30}$$

where β is defined to be the ratio $N_{pss}/N_{iss} < 1$, and it can be found as (see the Appendix):

$$\beta = \frac{N_{pss}}{N_{iss}} = \frac{1}{1 + \left(\frac{\mathbb{E}(T_0)}{T_s} - 2\right)\grave{P}_{fa} + \left(\frac{\mathbb{E}(T_1)}{T_s} - 2\right)\grave{P}_{md}}. \tag{31}$$

The expression obtained in (30) represents the PMF of the observed ISS idle periods resulting from Case I as shown in Fig. 4.

*2) **Case II**:* Another case where an idle period can be observed under ISS occurs between a single false alarm and the edge of the adjacent busy period as shown in Fig. 5. The probability of having such case is:

$$P(\breve{T}_0 = kT_s \mid \widehat{T}_0 \geq (k+1)T_s) = 2P_{fa}(1 - P_{fa})^k, \tag{32}$$

which is the probability of having a single false alarm and k non-false alarms in at least $k+1$ sensing events within an idle period. Note the presence of the factor of 2 because this case could occur at the left and right ends of an idle period next to a busy period. Therefore, following the same principle as in Case I, the unconditional PMF of such periods can be found by multiplying (32) by the ratio N^{II}_{pss}/N_{iss} as:

$$f^{II}_{\breve{T}_0}(\breve{T}_0 = kT_s) = \frac{2P_{fa}(1 - P_{fa})^k N^{II}_{pss}}{N_{iss}}, \tag{33}$$

where N^{II}_{pss} represents the number of periods observed under PSS with a duration ($\widehat{T}_0 \geq (k+1)T_s$), which is given by $N_{pss}\left(1 - F_{\widehat{T}_0}(kT_s)\right)$ where $F_{\widehat{T}_0}(kT_s)$ represents the Cumulative Distribution Function (CDF) of the idle periods observed under PSS. Thus, (33) can be written as:

$$\begin{aligned} f^{II}_{\breve{T}_0}(\breve{T}_0 = kT_s) &= \frac{2P_{fa}(1 - P_{fa})^k N_{pss}\left(1 - F_{\widehat{T}_0}(kT_s)\right)}{N_{iss}} \\ &= 2\beta P_{fa}(1 - P_{fa})^k \left(1 - F_{\widehat{T}_0}(kT_s)\right), \end{aligned} \tag{34}$$

The expression obtained in (34) represents the PMF of the observed ISS idle periods resulting from Case II as shown in Fig. 5.

*3) **Case III**:* The last case where an idle period can be observed under ISS occurs between two false alarms within the original idle period as shown in Fig. 6. The probability of having such case is:

$$P(\breve{T}_0 = kT_s \mid \widehat{T}_0 \geq (k+2)T_s) = \left(\frac{\widehat{T}_0}{T_s} - (k+1)\right) P^2_{fa}(1 - P_{fa})^k, \tag{35}$$

which is the probability to have two false alarms and k non-false alarms in at least $k+2$ sensing events within an idle period. For example, if $\widehat{T}_0 = (k+2)T_s$, the result of the above probability would be $P^2_{fa}(1 - P_{fa})^k$. Therefore, following the same principle as in Cases I and II, the unconditional PMF of such periods can be found as:

$$f^{III}_{\breve{T}_0}(\breve{T}_0 = kT_s) = \frac{\left(\frac{\sum_{n=1}^{N_{pss}} \widehat{T}^{III}_{0,n}}{T_s} - (k+1)N^{III}_{pss}\right) P^2_{fa}(1 - P_{fa})^k}{N_{iss}}, \tag{36}$$

where N^{III}_{pss} represents the number of periods observed under PSS with a duration ($\widehat{T}_0 \geq (k+2)T_s$) and $\sum_{n=1}^{N_{pss}} \widehat{T}^{III}_{0,n}$ is their summation. Thus, (36) can be written as (37).

The expression obtained in (37) represents the PMF of the observed ISS idle periods resulting from Case III as shown in Fig. 6.

The analysis presented so far has considered all the possible cases that can lead to the observation of an idle period under

$$f^{III}_{\check{T}_0}(\check{T}_0 = kT_s) = \frac{\left(\frac{\sum_{m=k+2}^{\infty}\left(mT_s f_{\widehat{T}_0}(\widehat{T}_0=mT_s)\right)N_{pss}}{T_s} - (k+1)N_{pss}\left(1-F_{\widehat{T}_0}((k+1)T_s)\right)\right)P^2_{fa}(1-P_{fa})^k}{N_{iss}}$$
$$= \frac{N_{pss}P^2_{fa}(1-P_{fa})^k}{N_{iss}}\left(\frac{\mathbb{E}(\widehat{T}_0) - \sum_{m=1}^{k+1}\left(mT_s f_{\widehat{T}_0}(\widehat{T}_0 = mT_s)\right)}{T_s} - (k+1)\left(1-F_{\widehat{T}_0}((k+1)T_s)\right)\right)$$
$$= \beta P^2_{fa}(1-P_{fa})^k\left(\frac{\mathbb{E}(\widehat{T}_0)}{T_s} - \sum_{m=1}^{k}\left(m f_{\widehat{T}_0}(\widehat{T}_0 = mT_s)\right) - (k+1)\left(1-F_{\widehat{T}_0}(kT_s)\right)\right). \quad (37)$$

$$f^{fa}_{\check{T}_0}(\check{T}_0 = kT_s) = \beta(1-P_{fa})^k\left[f_{\widehat{T}_0}(\widehat{T}_0 = kT_s) + 2P_{fa}\left(1-F_{\widehat{T}_0}(kT_s)\right) + P^2_{fa}\left(\frac{\mathbb{E}(\widehat{T}_0)}{T_s} - \sum_{m=1}^{k}\left(m f_{\widehat{T}_0}(\widehat{T}_0 = mT_s)\right) - (k+1)\left(1-F_{\widehat{T}_0}(kT_s)\right)\right)\right]. \quad (38)$$

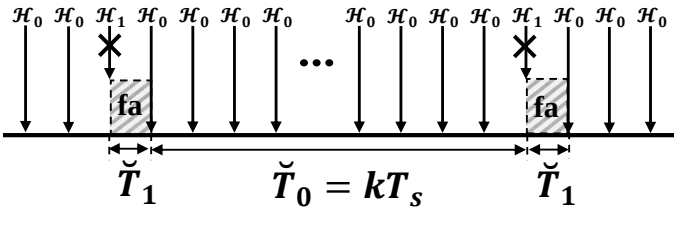

Fig. 6: Case III: An idle period $\check{T}_0 = kT_s$ observed between two false alarms.

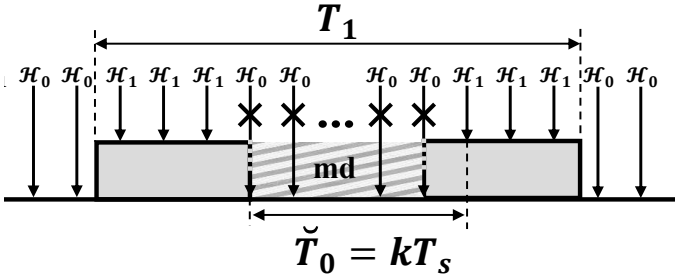

Fig. 7: An idle period $\check{T}_0 = kT_s$ observed within a busy period because of missed detections.

ISS (due to false alarms only) and the corresponding PMF was obtained for each case separately. Therefore, a general expression for the PMF that jointly considers the three cases can be obtained by combining (30), (34) and (37) as in (38).

The expression $f^{fa}_{\check{T}_0}(\check{T}_0 = kT_s)$ obtained in (38) represents the PMF of the periods observed under ISS as a function of the corresponding PMF, CDF, and mean period that would be estimated under PSS as well as the probability of false alarm and the sensing period. Since the missed detections were not considered in the previous analysis (i.e., $P_{md} = 0$), next section studies the effect of the missed detections on the calculation of the estimated distribution.

- ***Impact of missed detections:***

Under imperfect sensing, missed detections can also occur in the sensing decisions of the busy states of the channel, so that a busy state $\mathcal{H}_1$ can be incorrectly reported as an idle state $\mathcal{H}_0$. Therefore, any $\mathcal{H}_1$ sensing event within a T_1 period will have a probability of P_{md} to be misdetected, and a probability of $1-P_{md}$ not to be misdetected. Since there will be additional idle periods $\check{T}_0$ resulting from missed detections as shown in Fig. 7, we need to consider these periods as well when calculating the PMF of the idle periods. Therefore, the probability of observing an idle period within a busy period due to missed detections can be calculated as:

$$P(\check{T}_0 = kT_s \mid \widehat{T}_1 >= (k+2)T_s) = \left(\frac{\widehat{T}_1}{T_s} - (k+1)\right)P^k_{md}(1-P_{md})^2,$$

which is the probability to have k consecutive missed detections between two non-missed detections within at least $k+2$ sensing events of a busy period. Therefore, to find the PMF of such periods from a set $\{\widehat{T}_{1,n}\}_{n=1}^{N_{pss}}$ of N_{pss} busy periods the following can be yield:

$$f^{md}_{\check{T}_0}(\check{T}_0 = kT_s) = \frac{\left(\frac{\sum_{n=1}^{N_{pss}}\widehat{T}_{1,n}}{T_s} - (k+1)N_{pss}\right)P^k_{md}(1-P_{md})^2}{N_{iss}}$$
$$= \beta\left(\frac{\mathbb{E}(\widehat{T}_1)}{T_s} - (k+1)\right)P^k_{md}(1-P_{md})^2. \quad (39)$$

Note that the idle periods resulting from missed detections are more likely to occur as single periods (i.e., $k = 1$) than consecutive periods, and it is very unlikely that the whole sensing events of a busy period are missed detected. The obtained expression $f^{md}_{\check{T}_0}(\check{T}_0 = kT_s)$ in (39) represents the PMF of the idle periods observed under ISS (due to missed detections only).

- ***Final closed-form expression of the distribution:***

After analysing the impact of false alarms and missed detections on the estimation of the PMF of the idle periods observed under ISS, the final closed-form expression can be obtained by combining (38) with (39) as in (40). After simplifying (40), expression (41) is finally obtained.

The analytical result in (41) provides a closed-form relation between the PMF of the idle periods observed under ISS,

$$f_{\check{T}_0}(\check{T}_0 = kT_s) = \beta(1-P_{fa})^k \Bigg[f_{\widehat{T}_0}(\widehat{T}_0 = kT_s) + 2P_{fa}\left(1 - F_{\widehat{T}_0}(kT_s)\right) + P_{fa}^2 \left(\frac{\mathbb{E}(\widehat{T}_0)}{T_s} - \sum_{m=1}^{k} \left(m f_{\widehat{T}_0}(\widehat{T}_0 = mT_s) \right) - (k+1)\left(1 - F_{\widehat{T}_0}(kT_s)\right) \right) + \left(\frac{\mathbb{E}(\widehat{T}_1)}{T_s} - k - 1 \right) \frac{P_{md}^k (1-P_{md})^2}{(1-P_{fa})^k} \Bigg]. \tag{40}$$

$$f_{\check{T}_0}(\check{T}_0 = kT_s) = \Bigg[f_{\widehat{T}_0}(\widehat{T}_0 = kT_s) \left(\frac{P_{fa}^2 - 2P_{fa} + 1}{P_{fa}^2} \right) - \sum_{m=1}^{k-1} f_{\widehat{T}_0}(\widehat{T}_0 = mT_s) \left(m - k + \frac{2 - P_{fa}}{P_{fa}} \right) + \frac{\mathbb{E}(\widehat{T}_0)}{T_s} + \frac{2-P_{fa}}{P_{fa}} - k + \left(\frac{\mathbb{E}(\widehat{T}_1)}{T_s} - k - 1 \right) \frac{P_{md}^k (1-P_{md})^2}{P_{fa}^2 (1-P_{fa})^k} \Bigg] \beta P_{fa}^2 (1-P_{fa})^k. \tag{41}$$

$f_{\check{T}_0}(\check{T}_0 = kT_s)$, and the PMF $f_{\widehat{T}_0}(\widehat{T}_0 = kT_s)$, and the mean $\mathbb{E}(\widehat{T}_i)$ of the periods that would be estimated under PSS as well as the probabilities of sensing errors P_{fa} and P_{md}, and sensing period T_s. In other words, (41) satisfies the first stage of the analysis procedure mentioned in Section III. On the other hand, the expression of the estimated PMF under PSS, $f_{\widehat{T}_0}(\widehat{T}_0 = kT_s)$, as a function of the original PDF was provided in [23], which satisfies the second stage of the analysis mentioned in Section III. Therefore, by combining the second relationship with the first one, the relationship between the estimated PMF under ISS and the original PDF can then be achieved, which completes the third stage of the analysis mentioned in Section III.

B. Distribution Estimation Method

The closed-form expression in (41) suggests a novel method to accurately estimate the PMF of the channel periods under PSS, and therefore the original PDF, from the outcomes of the ISS estimates. Consequently, the analytical result in (41) can be solved for the PMF obtained under PSS $f_{\widehat{T}_0}(\widehat{T}_0 = kT_s)$ as a function of the PMF obtained under ISS $f_{\check{T}_0}(\check{T}_0 = kT_s)$, $\mathbb{E}(\check{T}_i)$, P_{fa}, P_{md} and T_s. This can be achieved by simplifying (41) as shown below:

$$f_{\check{T}_0}(\check{T}_0 = kT_s) = a_k \Bigg[c \cdot f_{\widehat{T}_0}(\widehat{T}_0 = kT_s) - \sum_{m=1}^{k-1} \left[f_{\widehat{T}_0}(\widehat{T}_0 = mT_s) \left(m - k + \frac{2-P_{fa}}{P_{fa}} \right) \right] + b_k \Bigg], \tag{42}$$

where

$$a_k = \beta P_{fa}^2 (1-P_{fa})^k, \tag{43a}$$

$$b_k = \frac{\mathbb{E}(\widehat{T}_0)}{T_s} + \frac{2-P_{fa}}{P_{fa}} - k + \left(\frac{\mathbb{E}(\widehat{T}_1)}{T_s} - k - 1 \right) \frac{P_{md}^k (1-P_{md})^2}{P_{fa}^2 (1-P_{fa})^k}, \tag{43b}$$

$$c = \left(\frac{P_{fa}^2 - 2P_{fa} + 1}{P_{fa}^2} \right). \tag{43c}$$

The equation shown in (42) can then be solved to find $f_{\widehat{T}_0}(\widehat{T}_0 = kT_s)$ as follows:

$$f_{\widehat{T}_0}(\widehat{T}_0 = kT_s) = \frac{1}{c} \Bigg[\frac{f_{\check{T}_0}(\check{T}_0 = kT_s)}{a_k} + \sum_{m=1}^{k-1} \left[f_{\widehat{T}_0}(\widehat{T}_0 = mT_s) \left(m - k + \frac{2-P_{fa}}{P_{fa}} \right) \right] - b_k \Bigg]. \tag{44}$$

Equation (44) can be used as a recursive formula (where $k \in \mathbb{N}^+$) whose initial value can be found for $k = 1$ and successive values can be found by iterating over k as shown in (45).

Note that the mean period $\mathbb{E}(\widehat{T}_i)$ in (43b) can be substituted with the corresponding mean estimator (24) proposed in Section V-D. As a result, the expression in (45) represents the estimator for the PMF of the periods that would be observed under PSS as a function of the PMF and mean obtained under ISS as well as P_{fa}, P_{md}, and T_s. Notice that the resulting PMF estimated from (45) is still a discrete distribution. A continuous estimation of the original distribution can be obtained by interpolating through the middle points of each discrete step in this PMF $f_{\widehat{T}_0}(\widehat{T}_0 = kT_s)$, which is justified by the analytical result obtained in [23, eq. (38)].

VIII. Numerical, Simulation and Experimental Results

In order to validate the analyses carried out in this work, we compare the results obtained from the numerical evaluation of the derived closed-form expressions with the counterpart obtained by means of both simulations and hardware experiments. Simulations are based on Matlab following a similar approach as in [31]. We generate a sequence of a sufficiently high number of idle/busy periods T_i with random durations drawn from a Generalised Pareto distribution (using $\mu_i = 10$ t.u., $\lambda_i = 30$ t.u. and $\alpha_i = 0.25$ as the values for the location, scale and shape parameters, see [31] for details). Then spectrum sensing is performed on the generated periods by employing a sensing period of T_s, using different values within the interval $(0, \mu_i)$. The calculated idle/busy periods from the

$$f_{\widehat{T}_0}(\widehat{T}_0 = kT_s) = \begin{cases} \dfrac{1}{c}\left[\dfrac{f_{\breve{T}_0}(\breve{T}_0 = kT_s)}{a_k} - b_k\right] & \text{for } k = 1 \\ \dfrac{1}{c}\left[\dfrac{f_{\breve{T}_0}(\breve{T}_0 = kT_s)}{a_k} + \displaystyle\sum_{m=1}^{k-1}\left[f_{\widehat{T}_0}(\widehat{T}_0 = mT_s)\left(m - k + \dfrac{2 - P_{fa}}{P_{fa}}\right)\right] - b_k\right] & \text{for } k > 1 \end{cases} \tag{45}$$

sensing decisions represent the corresponding sequence of periods $\widehat{T}_i$ that would be observed by a DSA/CR system under PSS. Introducing sensing errors on the PSS decisions, based on the selected value of P_{fa} and P_{md}, leads to the corresponding sequence of idle/busy periods $\breve{T}_i$ that would be observed under ISS. Finally, we can calculate the statistics of the periods $\breve{T}_i$ resulting from ISS and compare them with the original statistics of the generated periods T_i. The experimental results, on the other hand, are obtained by using a hardware Prototype for the Estimation of Channel Activity Statistics (PECAS). A detailed description of such prototype and its hardware and software implementations can be found in [39], where it was originally published. The transmitter, which represents the PU, generates a sequence of idle/busy periods from a Generalised Pareto distribution (similar to the simulations settings) and transmits 10^5 pairs of the generated idle/busy periods using a 433 MHz ON-OFF Keying (OOK) modulator with an output power of 2 dBm. The receiver, which represents the SU, uses a Software-Defined Radio (SDR) with a gain of 50 dB to observe the idle/busy activity at 433 MHz. Different sensing periods T_s (0 ms $< T_s <$ 10 ms) are employed by the SDR to sense the channel activity periodically. The receiver is placed sufficiently far away from the transmitter to ensure that the desired probability of missed detection is reached (further distance for higher probability of missed detection). The probability of false alarm is tuned by adjusting the energy decision threshold at the receiver. At each sensing event, samples are taken from the detected signal at a sampling rate of 10^6 samples/second for a duration of 3 ms. These samples are processed by an energy detection algorithm to decide the status of the channel (either idle or busy). Using the outcomes of the sensing decisions, the duration of the idle/busy periods can be estimated at the receiver side and their statistics can therefore be calculated. By comparing these statistics with the original statistics of the periods generated at the transmitter, the accuracy of the analytical results achieved in this work can be verified experimentally under realistic conditions and practical limitations of both transmitter and receiver. It is worth mentioning that the unit of the time used in the evaluation of the analytical expressions is given in a general form of time unit (t.u.). In the experimental scenario, however, where a specific unit needs to be selected, 1 ms is used as the reference time unit (i.e., 1 t.u. = 1 ms).

A. Estimation of the Minimum Period

The accuracy of the result in (2) for the estimated minimum period $\breve{\mu}_i$ under ISS was evaluated in [31] by means of simulations. We include here this evaluation for completeness and corroborate the simulation validation with experimental

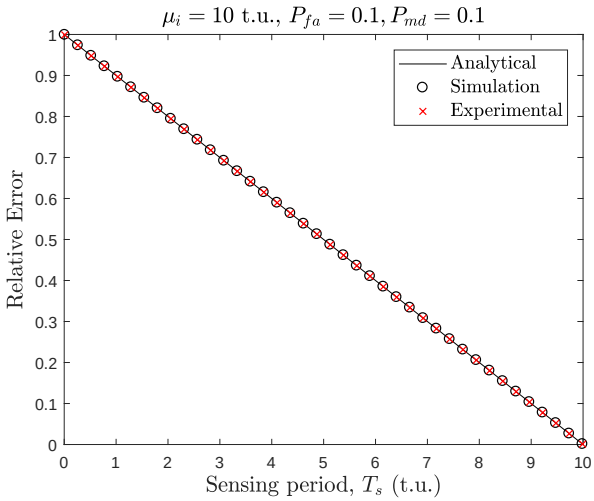

Fig. 8: Relative error of the calculated minimum period $\breve{\mu}_i$ under ISS.

results as well. The accuracy is evaluated by calculating the relative error of the estimated minimum idle period $\breve{\mu}_0$ under ISS with respect to its original value μ_0 as $|\breve{\mu}_0 - \mu_0|/\mu_0$. Assuming $\mu_0 = 10$ t.u. and $P_{fa} = P_{md} = 0.1$, the relative error can be found for different T_s values as shown in Fig. 8. The obtained results from simulations and experiments perfectly match the analytical expression given by (2), which thus corroborate its correctness and accuracy. It can also be noticed that as T_s increases the relative error decreases. This is because the estimated minimum period under ISS is $\breve{\mu}_0 = T_s$ and its value will approach the true minimum μ_0 as T_s tends to μ_0, thus making the relative error tend to zero accordingly. Same observations can also be noticed for any non-zero value of P_{fa} and P_{md} and they are also valid for the estimated minimum busy period $\breve{\mu}_1$ under ISS.

B. Estimation of the Mean Period

This section validates the analysis presented in Section V for the estimated mean period. First, Fig. 9 shows the relative error of the mean period estimated under ISS $\mathbb{E}(\breve{T}_i)$ with respect to the original mean period $\mathbb{E}(T_i)$ as a function of the employed sensing period. The results shown in Fig. 9 are obtained by numerically evaluating the analytical result in (17) as well as by means of simulations and hardware experiments, for both low ($P_{fa} = P_{md} = 0.01$) and high ($P_{fa} = P_{md} = 0.1$) probabilities of sensing errors. As it can be appreciated, there exists a perfect agreement among all three curves, thus demonstrating the accuracy of the closed-form expression obtained in (17) for the estimated mean period.

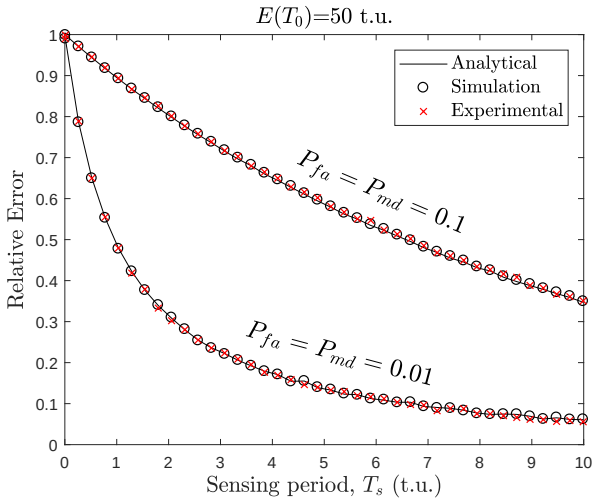

Fig. 9: Relative error of the calculated mean $\mathbb{E}(\check{T}_0)$ under ISS.

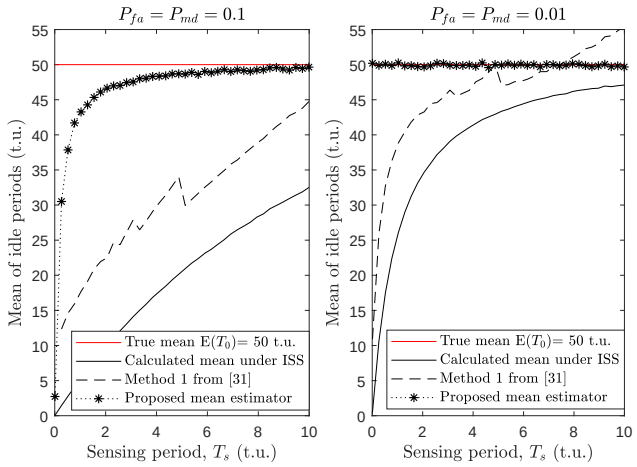

Fig. 10: Accuracy of the proposed mean estimator $\mathbb{E}(\widetilde{T}_i)$.

Fig. 10 compares the accuracy of the estimator for the mean period proposed in (24) with that attained by the conventional mean estimator shown in (4) as well as the best reconstruction algorithm proposed in [31] (named as Method 1 in [31], which discards the observed periods shorter than the minimum period μ_i). As it can be noticed, when the mean period is directly estimated from the channel periods observed under ISS based on (4), the resulting estimate is highly inaccurate. On the other hand, the proposed estimator in (24) provides a nearly perfect estimation under low probabilities of sensing errors ($P_{fa} = P_{md} = 0.01$) and a remarkable accuracy even under high probabilities of sensing errors ($P_{fa} = P_{md} = 0.1$), which approaches the exact mean period as the employed sensing period increases. In all cases, the proposed estimator will always provide more accurate results than the direct calculation and the reconstruction method of [31].

C. Estimation of the Duty Cycle

This section validates the analysis presented in Section VI for the estimated DC. Fig. 11 shows the relative error of the DC estimated under ISS when the estimation is obtained based on the conventional DC estimator (i.e., as the ratio of busy sensing decisions to the total number of sensing events) as well as the proposed DC estimator, which is based on mean period estimator in (24), a shown in (27). In addition, the proposed estimator is also compared with the best reconstruction algorithm from [31]. The results are shown for different combinations of low/high probabilities of sensing errors and for the whole range of possible DC values. In order to reproduce different DC values, the parameters of the Generalised Pareto distribution of idle periods is first configured as discussed at the beginning of Section VIII (i.e., $\mu_i = 10$ t.u., $\lambda_i = 30$ t.u. and $\alpha_i = 0.25$), which leads to a mean idle period of 50 t.u., while the scale and shape parameters of the Generalised Pareto distribution of busy periods (i.e., λ_1 t.u. and α_1) are adjusted (with $\mu_1 = 10$ t.u. kept constant) in order to provide the mean busy period required for the desired DC value. A sensing period of $T_s = 5$ t.u. is here considered for illustrative purposes but similar results are obtained for other values of the sensing period as well. As it can be clearly observed, the proposed DC estimator significantly outperforms the conventional method widely used in the literature to estimate the DC as well as the reconstruction method of [31] when a realistic scenario of ISS is considered. The relative error is almost zero in all cases, even when high probabilities of sensing errors are considered (e.g., $P_{fa} = P_{md} = 0.1$ in Fig. 11(a)). The excellent level of accuracy achieved by the proposed DC estimation approach, even in the presence of severe probabilities of sensing errors, highlights its practical utility in realistic scenarios.

D. Estimation of the Distribution

This section validates the analysis presented in Section VII for the estimated distribution. Fig. 12 compares the theoretical expression in (41) for the PMF of the periods observed under ISS with the equivalent results obtained from simulations and hardware experiments. As it can be observed, there is a perfect agreement for all the considered cases shown in Fig. 12. A more quantitative comparison can be performed based on the well-known Kolmogorov-Smirnov (KS) distance [40], which in the context of this work is defined as the maximum absolute difference between the CDF of the periods observed under ISS, and the CDF of the original periods:

$$D_{KS} = \sup_{kT_s} \mid F_{T_i}(kT_s) - F_{\check{T}_i}(kT_s) \mid, \text{ where } k \in \mathbb{N}^+. \quad (46)$$

While the original period durations T_i and their CDF $F_{T_i}(\cdot)$ can be assumed to be continuous in general, the periods observed under ISS $\check{T}_i$ are integer multiple values of the employed sensing period and therefore their CDF $F_{\check{T}_i}(\cdot)$ is discrete. In order to enable the comparison between these continuous and discrete distributions based on (46), the continuous distribution $F_{T_i}(\cdot)$ is evaluated at discrete points for which $F_{\check{T}_i}(\cdot)$ is defined (i.e., $T_i = kT_s$, $k \in \mathbb{N}^+$). The KS distance as defined in the context of this work in (46) is first evaluated numerically based on (41) and then compared to the corresponding KS distance obtained from simulations and hardware experiments. The results are shown in Fig. 13 for different DC values and probabilities of sensing errors. As it can be observed,

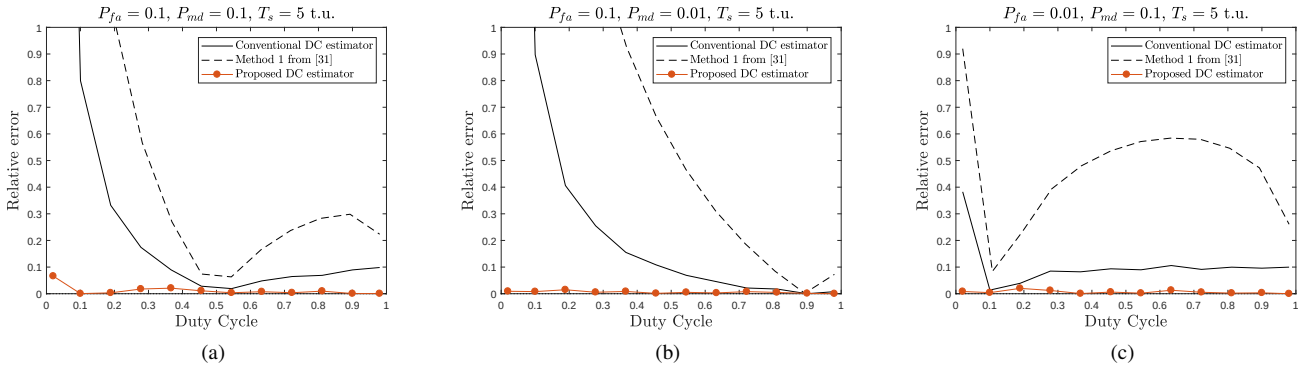

Fig. 11: Relative error of the proposed DC estimator $\widetilde{\Psi}$ for different P_{fa} and P_{md} (T_s = 5 t.u.).

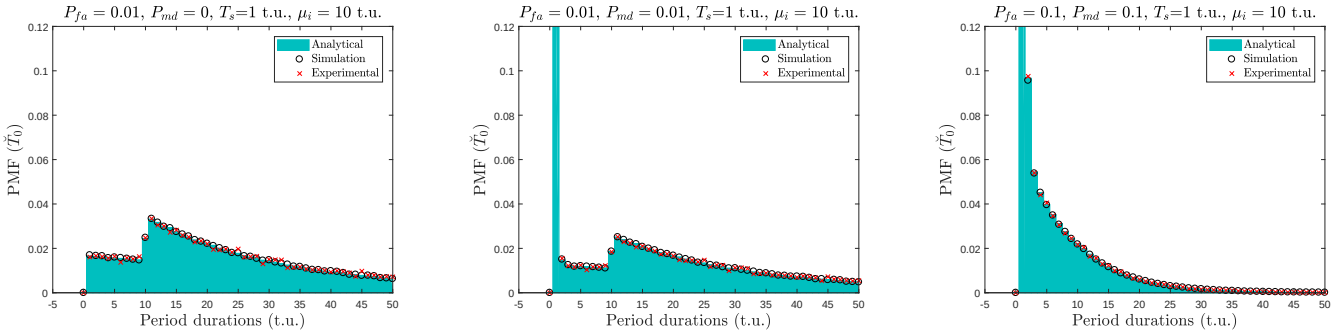

Fig. 12: Estimating the PMF of the idle periods under ISS using different probabilities of error and when T_s = 1 t.u..

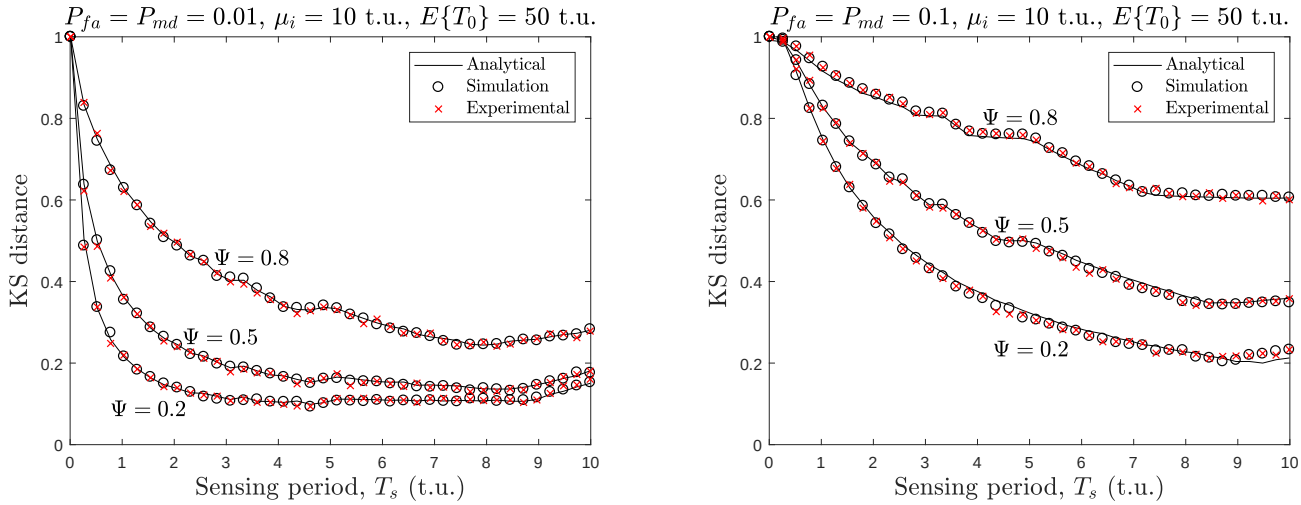

Fig. 13: KS distance of the calculated distribution under ISS as a function of the sensing period for different DC values and probabilities of sensing errors.

there is a perfect agreement among analytical, simulation and experimental results, which validates the theoretical expression obtained in (41).

In the same way we can examine the accuracy of the novel estimator proposed in (45) to estimate the true distribution of the periods observed under ISS. The proposed estimator finds the PSS distribution from the ISS observations, which in turn can be used to find the original distribution as detailed in [23]. Therefore, by comparing the KS distance of the proposed estimator with the KS distance resulting from the direct estimation under ISS (without using any estimation method), the improvement of the proposed estimation approach can be assessed. As it can be appreciated in Fig. 14, the proposed estimator leads to a significantly improved accuracy in the estimation of the true distribution of the periods based on the ISS outcomes, providing a nearly perfect estimation ($D_{KS} \approx 0$) under low sensing error probability and a significantly more accurate estimation even under high

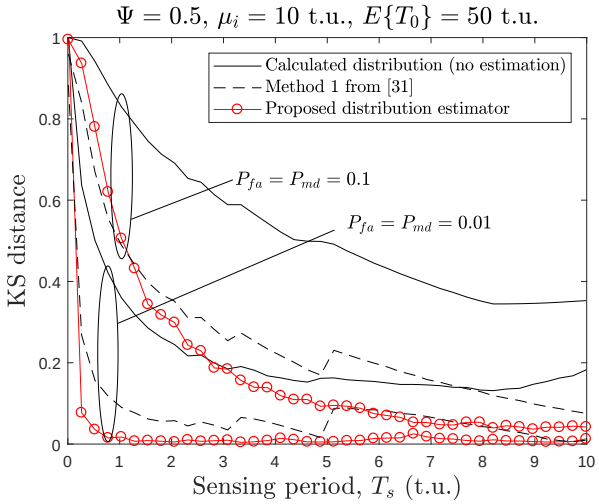

Fig. 14: KS distance of the proposed distribution estimator.

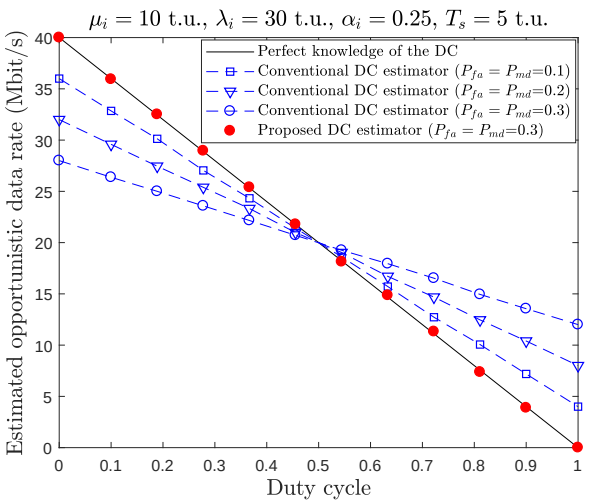

Fig. 15: Estimated opportunistic data rate under ISS as a function of the DC.

error probability (provided that the appropriate sensing period is selected). In addition, the proposed estimator outperforms the best reconstruction algorithm proposed in [31]. These results highlight the feasibility of obtaining a highly accurate estimation of the primary channel activity statistics from spectrum sensing observations, even in the presence of sensing errors, if the methods proposed in this work are employed.

E. Illustrative example

The purpose of this section is to show how the estimation accuracy of the primary channel activity statistics significantly affects the performance of the DSA/CR system. In this illustrative example the problem of estimating the opportunistic data rate that is available in the primary channels is considered. Data rate estimation can help DSA/CR systems select the most attractive (highest opportunistic data rate) primary channel that can be offered to the SUs. The opportunistic data rate R_b can be calculated from the primary channel duty cycle Ψ, channel bandwidth W and spectrum efficiency η (based on the modulation and coding schemes used by the DSA/CR system) as $R_b = (1 - \Psi)W\eta$. As discussed in Section VI, the channel DC can not be estimated accurately under ISS using the conventional method, thus providing an inaccurate estimation for the data rate as well, as $\breve{R}_b = (1 - \breve{\Psi})W\eta$. In contrast, accurate estimation under ISS can be achieved using the proposed DC estimator in (27), which in turn provides accurate estimation for the data rate $\widetilde{R}_b = (1 - \widetilde{\Psi})W\eta$ as well. Fig. 15 shows the estimated data rate under ISS (assuming $W = 20$ MHz and $\eta = 2$ bit/s/Hz) as a function of the DC using the conventional method as well as the proposed method, which are both compared with the estimated data rate assuming a perfect knowledge of the DC as a reference. As it can be noticed, when the channel DC is lower than 0.5, the conventional method would underestimate the actual available data rate in the primary channel as the probability of sensing error increases (which results in significant waste of free capacity in the primary channel). In addition, when the channel DC is greater than 0.5, the conventional method would overestimate the actual available data rate in the primary channel as the probability of sensing error increases (which results in significant shortage of free capacity than expected in the primary channel). On the other hand, the proposed DC estimator can provide a perfect estimation of the available opportunistic data rate even under severe ISS ($P_{fa} = P_{md} = 0.3$). As a result, a more efficient exploitation of the frequency spectrum can be achieved. This illustrative example shows how inaccurate estimation of the primary channel activity statistics under ISS can severely impact the performance of the DSA/CR systems, and it highlights the importance of the achieved analytical results in this work to provide accurate estimations for primary channel statistics.

IX. Conclusion

Primary channel activity statistics can play an important role in enhancing the performance of DSA/CR systems. However, in practice these statistics can be severely corrupted by sensing errors under ISS to the extent that they would not be of any practical use in DSA/CR systems. Therefore, studying analytically the impact of sensing errors on statistics estimation can help understand how their degrading effects can be overcome. This work has derived a set of closed-form expressions for a variety of primary channel statistics, which establish the relationship between the statistics estimated under ISS and their corresponding original values, as a function of the parameters used by the DSA/CR system to configure the spectrum sensing operation (i.e., probability of error and sensing period). Furthermore, this work has proposed a set of novel estimators for the studied primary channel statistics, which have been proven by means of simulations and hardware experiments to outperform the existing estimators widely used in the literature and are able to provide highly accurate (nearly perfect) estimations under ISS even under high probability of sensing errors. The outcomes of this work will enable DSA/CR systems to exploit a different range of primary channel statistics, not only under PSS, but also under realistic

spectrum sensing conditions (i.e., ISS), which in turn will open further opportunities for possible future applications.

APPENDIX A
Calculation of the ratio β given in (31)

The ratio $\beta = N_{pss}/N_{iss}$ can be derived as follows:

$$\beta = \frac{N_{pss}}{N_{iss}} = \frac{N_{pss}}{N_{pss} + N_{fa} + N_{md}}. \tag{47}$$

As explained in Case I and Case II of Section V, sensing errors will not always produce additional periods. The number of errors (N_{fa} and N_{md}) that could result in additional periods is found as:

$$N_{fa} = \left(\frac{\sum_{n=1}^{N_{pss}} \widehat{T}_{0,n}}{T_s} - 2N_{pss} \right) \grave{P}_{fa}, \tag{48}$$

$$N_{md} = \left(\frac{\sum_{n=1}^{N_{pss}} \widehat{T}_{1,n}}{T_s} - 2N_{pss} \right) \grave{P}_{md}. \tag{49}$$

Equations (48) and (49) are similar to (6) and (8) but after considering Case I and Case II of Section V. Furthermore, (10) can be used to simplify (48) and (49) to yield:

$$N_{fa} = N_{pss} \left(\frac{\widehat{m}_0}{T_s} - 2 \right) \grave{P}_{fa}, \tag{50}$$

$$N_{md} = N_{pss} \left(\frac{\widehat{m}_1}{T_s} - 2 \right) \grave{P}_{md}. \tag{51}$$

Taking into account that $\widehat{m}_i$ can be replaced by $\mathbb{E}(T_i)$ (as explained in Section V-C) and substituting (50) and (51) into (47), we can finally obtain the result presented in (31).

REFERENCES

[1] Ofcom, "The Future Role of Spectrum Sharing for Mobile and Wireless Data Services," Ofcom Statement, Apr. 2014.

[2] Federal Communications Commission (FCC), Spectrum Policy Task Force, "Report of the spectrum efficiency working group," Nov. 2002.

[3] Q. Zhao and B. M. Sadler, "A survey of dynamic spectrum access," *IEEE Signal Process. Mag.*, vol. 24, no. 3, pp. 79–89, May 2007.

[4] M. López-Benítez, "Cognitive radio," in *Heterogeneous cellular networks: Theory, simulation and deployment.* Cambridge University Press, 2013, ch. 13.

[5] H. Urkowitz, "Energy detection of unknown deterministic signals," *Proc. IEEE*, vol. 55, no. 4, pp. 523–531, Apr. 1967.

[6] M. López-Benítez and F. Casadevall, "Improved energy detection spectrum sensing for cognitive radio," *IET Communications*, vol. 6, no. 8, pp. 785–796, 22 May 2012.

[7] C. Vladeanu, C. Nastase and A. Martian, "Energy Detection Algorithm for Spectrum Sensing Using Three Consecutive Sensing Events," *IEEE Wireless Communications Letters*, vol. 5, no. 3, pp. 284–287, June 2016.

[8] J. Chen, X. Ge and Q. Ni, "Coverage and Handoff Analysis of 5G Fractal Small Cell Networks," *IEEE Transactions on Wireless Communications*, vol. 18, no. 2, pp. 1263–1276, Feb. 2019.

[9] X. Ge, X. Tian, Y. Qiu, G. Mao and T. Han, "Small-Cell Networks With Fractal Coverage Characteristics," *IEEE Transactions on Communications*, vol. 66, no. 11, pp. 5457–5469, Nov. 2018.

[10] X. Ge et al., "Wireless fractal cellular networks," *IEEE Wireless Comms*, vol. 23, no. 5, pp. 110–119, October 2016.

[11] G. Ding *et al.*, "Spectrum Inference in Cognitive Radio Networks: Algorithms and Applications," in *IEEE Communications Surveys & Tutorials*, vol. 20, no. 1, pp. 150–182, Firstquarter 2018.

[12] L. Yang, N. Lv, and Z. X. Xu, "Spectrum prediction for cognitive radio system based on optimally pruned extreme learning machine," *Appl. Mech. Mater.*, vols. 536–537, pp. 430–436, Apr. 2014.

[13] Y. Chen and H.-S. Oh, "Spectrum measurement modelling and prediction based on wavelets," *IET Communications*, vol. 10, no. 16, pp. 2192–2198, Oct 2016.

[14] X. Xing, T. Jing, W. Cheng, Y. Huo, and X. Cheng, "Spectrum prediction in cognitive radio networks," *IEEE Wireless Commun.*, vol. 20, no. 2, pp. 90–96, Apr. 2013.

[15] K. Umebayashi, K. Hayashi and J. J. Lehtomäki, "Threshold-Setting for Spectrum Sensing Based on Statistical Information," in *IEEE Communications Letters*, vol. 21, no. 7, pp. 1585–1588, July 2017.

[16] S. Sengottuvelan, J. Ansari, P. Mähönen, T. G. Venkatesh and M. Petrova, "Channel Selection Algorithm for Cognitive Radio Networks with Heavy-Tailed Idle Times," in *IEEE Trans. on Mobile Computing*, vol. 16, no. 5, pp. 1258–1271, 2017.

[17] M. B. Hosen, M. M. H. Mridha and M. A. Hamza, "Secondary User Channel Selection in Cognitive Radio Network Using Adaptive Method," *2018 3rd International Conference for Convergence in Technology (I2CT)*, Pune, 2018, pp. 1–6.

[18] X. Liu, B. Krishnamachari, and H. Liu, "Channel selection in multichannel opportunistic spectrum access networks with perfect sensing," in *Proc. 2010 IEEE Int'l. Symp. Dyn. Spect. Access Networks (DySPAN 2010)*, Apr. 2010, pp. 1–8.

[19] A. John and A. P. Mathew, "Channel selection in cognitive radio networks using exploration order and stopping rule," *2016 International Conference on Communication and Electronics Systems (ICCES)*, Coimbatore, 2016, pp. 1–5.

[20] G. C. Deepak, K. Navaie and Q. Ni, "Radio Resource Allocation in Collaborative Cognitive Radio Networks Based on Primary Sensing Profile," in *IEEE Access*, vol. 6, pp. 50344–50357, 2018.

[21] W. Zhang, C. Wang, X. Ge and Y. Chen, "Enhanced 5G Cognitive Radio Networks Based on Spectrum Sharing and Spectrum Aggregation," in *IEEE Trans. on Comms.*, vol. 66, no. 12, pp. 6304–6316, Dec. 2018.

[22] E. Jung and X. Liu, "Opportunistic spectrum access in multiple-primary-user environments under the packet collision constraint," *IEEE/ACM Trans. Networking*, vol. 20, no. 2, pp. 501–514, Apr. 2012.

[23] M. López-Benítez, A. Al-Tahmeesschi, D. Patel, J. Lehtomäki and K. Umebayashi, "Estimation of Primary Channel Activity Statistics in Cognitive Radio Based on Periodic Spectrum Sensing Observations," in *IEEE Transactions on Wireless Communications*, vol. 18, no. 2, pp. 983–996, Feb. 2019.

[24] M. López-Benítez and J. Lehtomäki, "Energy detection based estimation of primary channel occupancy rate in cognitive radio," *2016 IEEE Wireless Communications and Networking Conference*, Doha, 2016, pp. 1–6.

[25] J. Lehtomäki, M. López-Benítez, K. Umebayashi and M. Juntti, "Improved Channel Occupancy Rate Estimation," in *IEEE Transactions on Communications*, vol. 63, no. 3, pp. 643–654, March 2015.

[26] J. J. Lehtomaki, R. Vuohtoniemi and K. Umebayashi, "On the Measurement of Duty Cycle and Channel Occupancy Rate," in *IEEE Journal on Selected Areas in Communications*, vol. 31, no. 11, pp. 2555–2565, November 2013.

[27] W. Gabran, P. Pawelczak, C. Liu and D. Cabric, "Blind estimation of primary user traffic parameters under sensing errors," *2013 IEEE International Conference on Communications (ICC)*, Budapest, 2013, pp. 2391–2396.

[28] W. Gabran, C. H. Liu, P. Pawelczak and D. Cabric, "Primary user traffic estimation for dynamic spectrum access," *IEEE Journal on Selected Areas in Communications*, vol. 31, no. 3, pp. 544–558, March 2013.

[29] Q. Liang, M. Liu and D. Yuan, "Channel Estimation for Opportunistic Spectrum Access: Uniform and Random Sensing," in *IEEE Transactions on Mobile Computing*, vol. 11, no. 8, pp. 1304–1316, Aug. 2012.

[30] M. López-Benítez, and F. Casadevall, "Time-dimension models of spectrum usage for the analysis, design, and simulation of cognitive radio networks," *IEEE Trans. Veh. Tech.*, vol. 62, no. 5, pp. 2091–2104, Jun 2013.

[31] M. López-Benítez, "Can primary activity statistics in cognitive radio be estimated under imperfect spectrum sensing?" in *Proc. 24th Annual IEEE Int'l. Symp. Pers., Indoor and Mobile Radio Comms. (PIMRC 2013)*, Sep. 2013, pp. 750–755.

[32] A. Al-Tahmeesschi, M. López-Benítez, J. Lehtomäki and K. Umebayashi, "Investigating the Estimation of Primary Occupancy Patterns under Imperfect Spectrum Sensing," *2017 IEEE Wireless Communications and Networking Conference Workshops (WCNCW)*, San Francisco, CA, 2017, pp. 1–6.

[33] A. Al-Tahmeesschi, M. López-Benítez, J. Lehtomäki and K. Umebayashi, "Improving primary statistics prediction under imperfect spectrum sensing," *2018 IEEE Wireless Comms. and Networking Conference (WCNC)*, Barcelona, 2018, pp. 1–6.

[34] A. Al-Tahmeesschi, M. López-Benítez, D. K. Patel, J. Lehtomäki and K. Umebayashi, "On the Sample Size for the Estimation of Primary Activity Statistics Based on Spectrum Sensing," in *IEEE Transactions on Cognitive Communications and Networking*, vol. 5, no. 1, pp. 59–72, March 2019.
[35] M. López-Benítez and F. Casadevall, "Methodological aspects of spectrum occupancy evaluation in the context of cognitive radio," *European Trans. Telecommun.*, vol. 21, no. 8, pp. 680–693, Dec. 2010.
[36] A. D. Spaulding and G. H. Hagn, "On the definition and estimation of spectrum occupancy," *IEEE Trans. Electromagn. Compat.*, vol. 19, no. 3, pp. 269–280, Aug. 1977.
[37] M. Wellens and P. Mähönen, "Lessons learned from an extensive spectrum occupancy measurement campaign and a stochastic duty cycle model," *Mobile Netw. Appl.*, vol. 15, no. 3, pp. 461–474, 2010.
[38] A. Al-Tahmeesschi, M. López-Benítez, K. Umebayashi and J. Lehtomäki, "Analytical study on the estimation of primary activity distribution based on spectrum sensing," *2017 IEEE 28th Annual International Symposium on Personal, Indoor, and Mobile Radio Communications (PIMRC)*, Montreal, QC, 2017, pp. 1–5.
[39] M. López-Benítez, A. Al-Tahmeesschi, K. Umebayashi and J. Lehtomäki, "PECAS: A low-cost prototype for the estimation of channel activity statistics in cognitive radio," in *Proc. IEEE Wirel. Comms. and Net. Conf. (WCNC 2017)*, 2017, pp. 1–6.
[40] W. H. Press, S. A. Teukolsky, W. T. Vetterling, and B. P. Flannery, *Numerical recipes: The art of scientific computing*, 3rd ed. Cambridge University Press, 2007.

Ogeen H. Toma (S'16) received the B.Sc. degree in electrical and computer engineering from the University of Duhok, Iraq, in 2011, and the M.Sc. degree in wireless communications (with distinction) from the University of Southampton, U.K., in 2015. He is currently pursuing the Ph.D. degree with the department of electrical engineering and electronics, University of Liverpool, U.K., under the UK-India Education and Research Initiative (UKIERI) DST Thematic Partnerships Programme. His research interests include 5G wireless communications, cognitive radio, dynamic spectrum access, spectrum sensing, statistics estimation, cooperative wireless communications, MIMO and massive MIMO systems.

Miguel López-Benítez (S'08, M'12, SM'17) received the B.Sc. and M.Sc. degrees (both First-Class with Distinction) in Telecommunication Engineering from Miguel Hernández University, Elche, Spain in 2003 and 2006, respectively, and the Ph.D. degree (*summa cum laude*) in Telecommunication Engineering from the Technical University of Catalonia, Barcelona, Spain in 2011. From 2011 to 2013, he was a Research Fellow with the Centre for Communication Systems Research, University of Surrey, Guildford, U.K. In 2013, he became a Lecturer (Assistant Professor) with the Department of Electrical Engineering and Electronics, University of Liverpool, U.K., where he was promoted to Senior Lecturer (Associate Professor) in 2018, which is his current position.

His research interests include the field of wireless communications and networking, with special emphasis on cellular mobile communications and dynamic spectrum access in cognitive radio systems. He has been the Principal Investigator or Co-Investigator of research projects funded by the EPSRC, British Council, and Royal Society. He has also been involved in the European-funded projects AROMA, NEWCOM++, FARAMIR, QoSMOS, and CoRaSat. He is an Associate Editor of IEEE Access, IET Communications, and Wireless Communications and Mobile Computing, and has been a member of the Organising Committee for the IEEE WCNC International Workshop on Smart Spectrum since 2015. Please visit http://www.lopezbenitez.es for more details.

Dhaval K. Patel is currently working as an Assistant Professor at School of Engineering and Applied Science - Ahmedabad University, India since 2014. He was also a visiting faculty at Franklin W. Olin College of Engineering-Massachusetts, USA. He worked as Junior Research Fellow in the Post Graduate Lab for Communication Systems at the Nirma University-India from 2011 to 2014. He received the B.E. and M.E. degrees in Communication Systems Engineering (both with Distinction/First-Class) from Gujarat University in 2003 and 2010, respectively, and a Ph.D. degree in Electronics and Communications from the Institute of Technology-Nirma University, India in 2014. His research area of interest includes Vehicular Cyber Physical System, 5G Wireless Networks, Non-parametric statistics and Physical Layer Security. He is the principal investigator of research projects funded by Department of Science and Technology (DST), UK-India Education and Research Initiative (UKIERI), Association of Southeast Asian Nations (ASEAN)-India Collaborative R&D Project and Gujarat Council on Science and Technology (GUJCOST). He serves as a reviewer in various conferences including IEEE ICASSP, IEEE VTC and IEEE PIMRC.

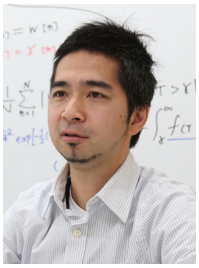

Kenta Umebayashi (S'00–M'04) received the B.E., M.E., and Ph.D. degrees from Yokohama National University, Japan, in 1999, 2001, and 2004, respectively, and the LL.B. degree from Ritsumeikan University, Japan, in 1996. From 2004 to 2006, he was a Research Scientist with the Centre for Wireless Communications, University of Oulu, Finland. He is currently an Associate Professor with the Tokyo University of Agriculture and Technology, Japan. He was a Principal Investigator of four grants-in-aid for scientific research projects and three strategic information and communications research and development promotion programme projects including a HORIZON 2020 project. His research interests lie in the areas of signal detection and estimation theories for wireless communication, signal processing for multiple antenna systems, cognitive radio networks, and terahertz band wireless communications. He received the Best Paper Award at the 2012 IEEE WCNC and the Best Paper Award at the 2015 IEEE WCNC Workshop from IWSS.